

Online Supplementary

Supplementary Methods

Supplementary Tables and Figures

Figure S1. Meta-regression of Global Metric Effect Sizes on Mean Age

Figure S2. Funnel Plot of Global Topological Metrics

Figure S3. Leave-one-out Influence Analysis of Global Topological Metrics

Figure S4. Meta-regression of Local Metric Effect Sizes on Mean Age

Table S1. Definition of Topological Metrics

Table S2. Quality Assessment of Included Studies

Table S3. Sensitivity Analysis of Variance Estimators for Global Metric Pooling

Table S4. Funnel Plots and Bias Analyses in Regions with Hubness Alteration

Supplementary Methods

1. Literature search

Based on our pre-registered protocol (registration doi: [10.17605/OSF.IO/TKX2P](https://doi.org/10.17605/OSF.IO/TKX2P)), a systematic literature search was conducted across PubMed, Web of Science, and Embase to identify articles investigating graph theory analysis in ADHD published from January 1, 2009 to February 21, 2025. The following search terms were used: ("ADHD" OR "attention-deficit/hyperactivity disorder" OR "hyperkinetic") AND ("connectom*" OR "graph theor*" OR "graph metric*" OR "graph analys*" OR "network analys*" OR "topolog*" OR "brain connectivity" OR "small-world*" OR "modularity") AND ("MRI" OR "magnetic resonance imaging" OR "DTI" OR "diffusion tensor imaging" OR "dMRI" OR "fMRI" OR "rs-fMRI" OR "structural MRI"). These terms were searched in all available fields in each database, and Boolean operators (AND/OR) were used to combine the terms across three conceptual domains: disorder, network analysis method, and neuroimaging modality.

2. Quality assessment

Category 1: Subjects

1. Patients were evaluated prospectively, specific diagnostic criteria were applied, and demographic data was reported.
2. Neurotypical control subjects were evaluated prospectively, psychiatric and medical illnesses were excluded, and demographic data was reported.
3. Important variables (e.g. illness duration, severity of illness, drug status, handedness) were checked either by stratification or statistically.
4. Sample size per group > 10, and no significant difference in age and sex existed.

Category 2: Methods for image acquisition and analysis

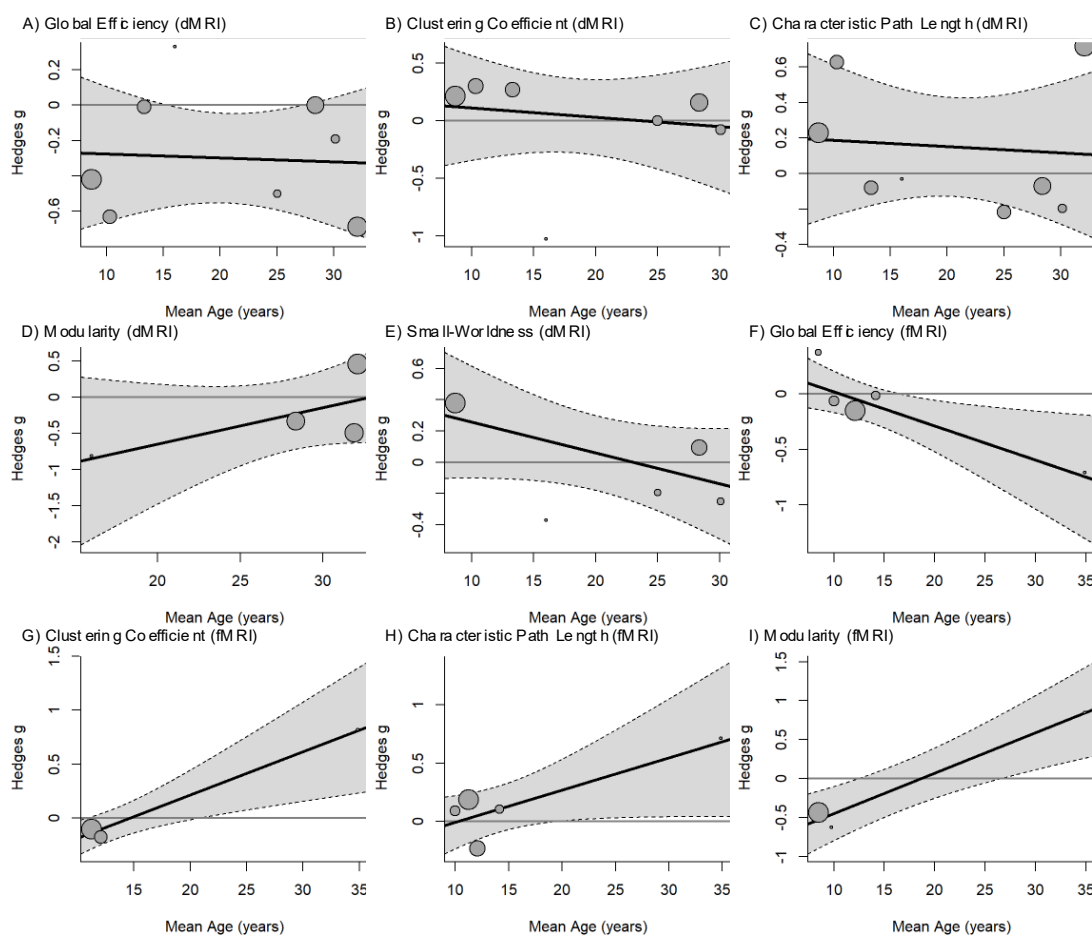
5. Magnet strength was at least 3.0T.
6. DTI with at least 30 directions was used.
7. The imaging technique used was clearly described and is reproducible.
8. Parcellation scheme was clearly reported, and no brain regions were excluded from the parcellation.

9. Calculation of graph metrics were clearly described and are reproducible, with both global and nodal findings provided.

Category 3: Results and conclusions

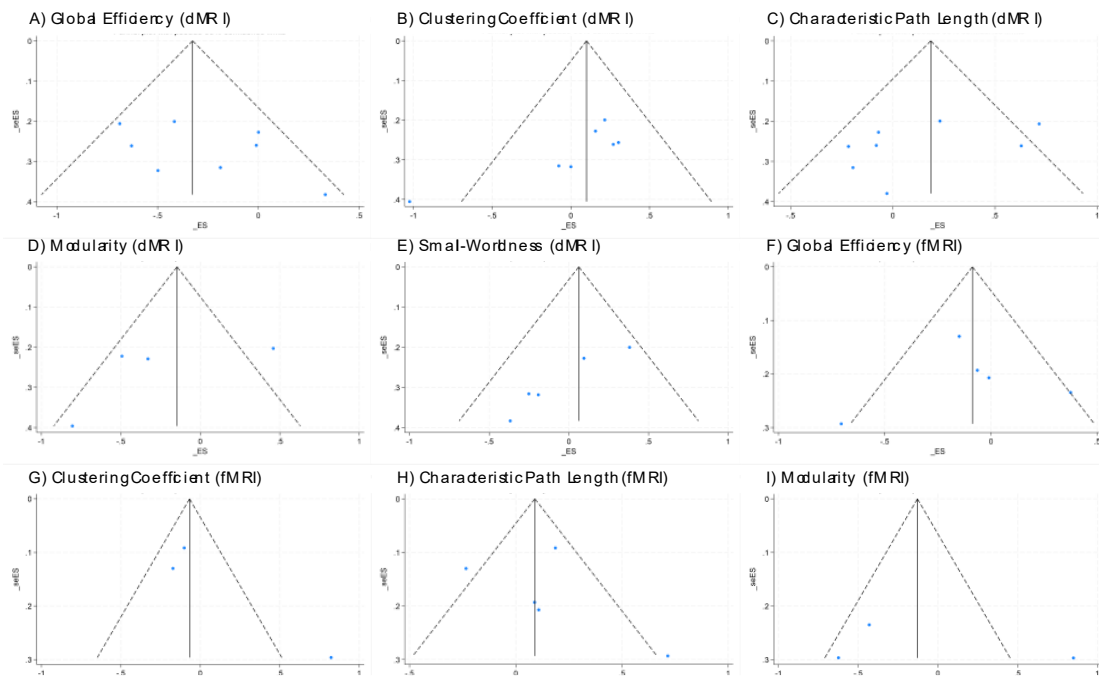
10. Corrections for multiple comparisons (if necessary).
11. Statistical parameters for significant and important non-significant differences were provided.
12. Conclusions were consistent with the results obtained, and limitations were discussed.

Figure S1. Meta-regression of Global Metric Effect Sizes on Mean Age



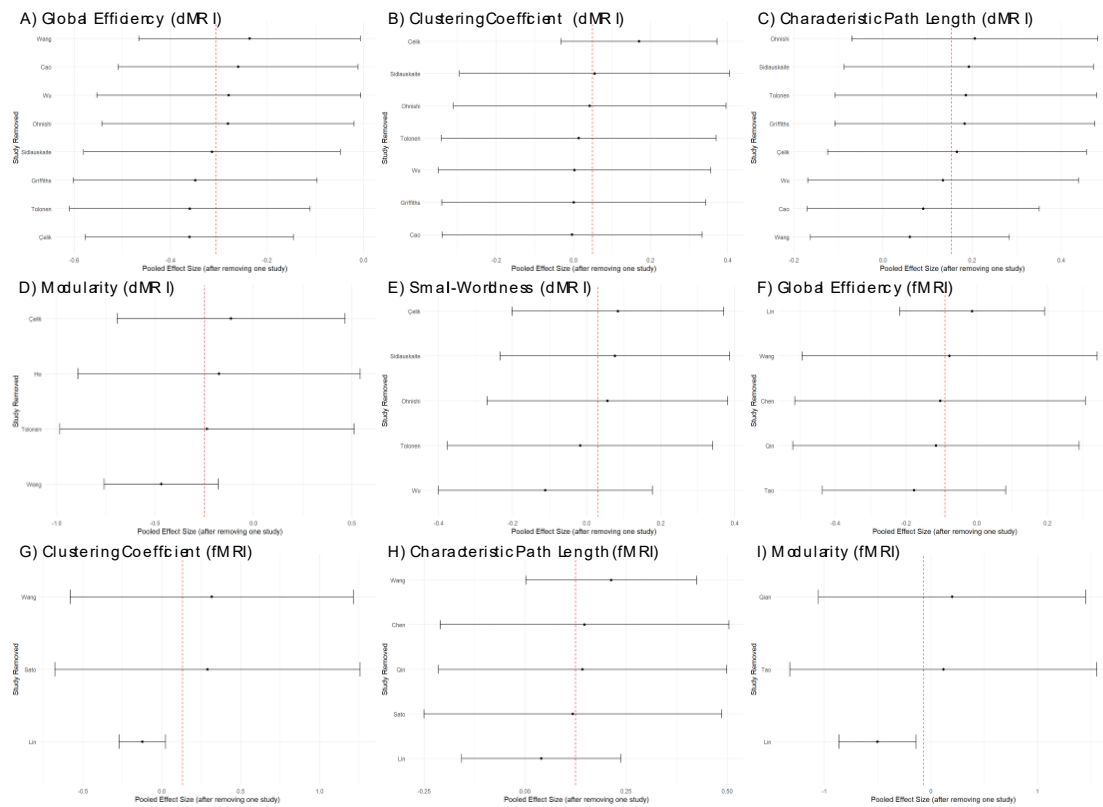
(A–E) Bubble plots showing the meta-regression of effect sizes for dMRI network metrics against the mean age of study populations. The metrics include (A) Global Efficiency ($\beta = -0.002$, $p = .87$), (B) Clustering Coefficient ($\beta = -0.008$, $p = .68$), (C) Characteristic Path Length ($\beta = -0.004$, $p = .82$), (D) Modularity ($\beta = 0.050$, $p = .23$), and (E) Small-Worldness ($\beta = -0.020$, $p = .14$). (F–I) Bubble plots showing the meta-regression of effect sizes for fMRI network metrics against the mean age of study populations. The metrics include (F) Global Efficiency ($\beta = -0.031$, $p = .02$), (G) Clustering Coefficient ($\beta = 0.040$, $p = .02$), (H) Characteristic Path Length ($\beta = 0.028$, $p = .06$), and (I) Modularity ($\beta = 0.052$, $p = .00$). Note. The solid line represents the fitted regression line, and the shaded area indicates the 95% confidence interval. Circle size reflects the weight of each study in the meta-analysis.

Figure S2. Funnel Plot of Global Topological Metrics



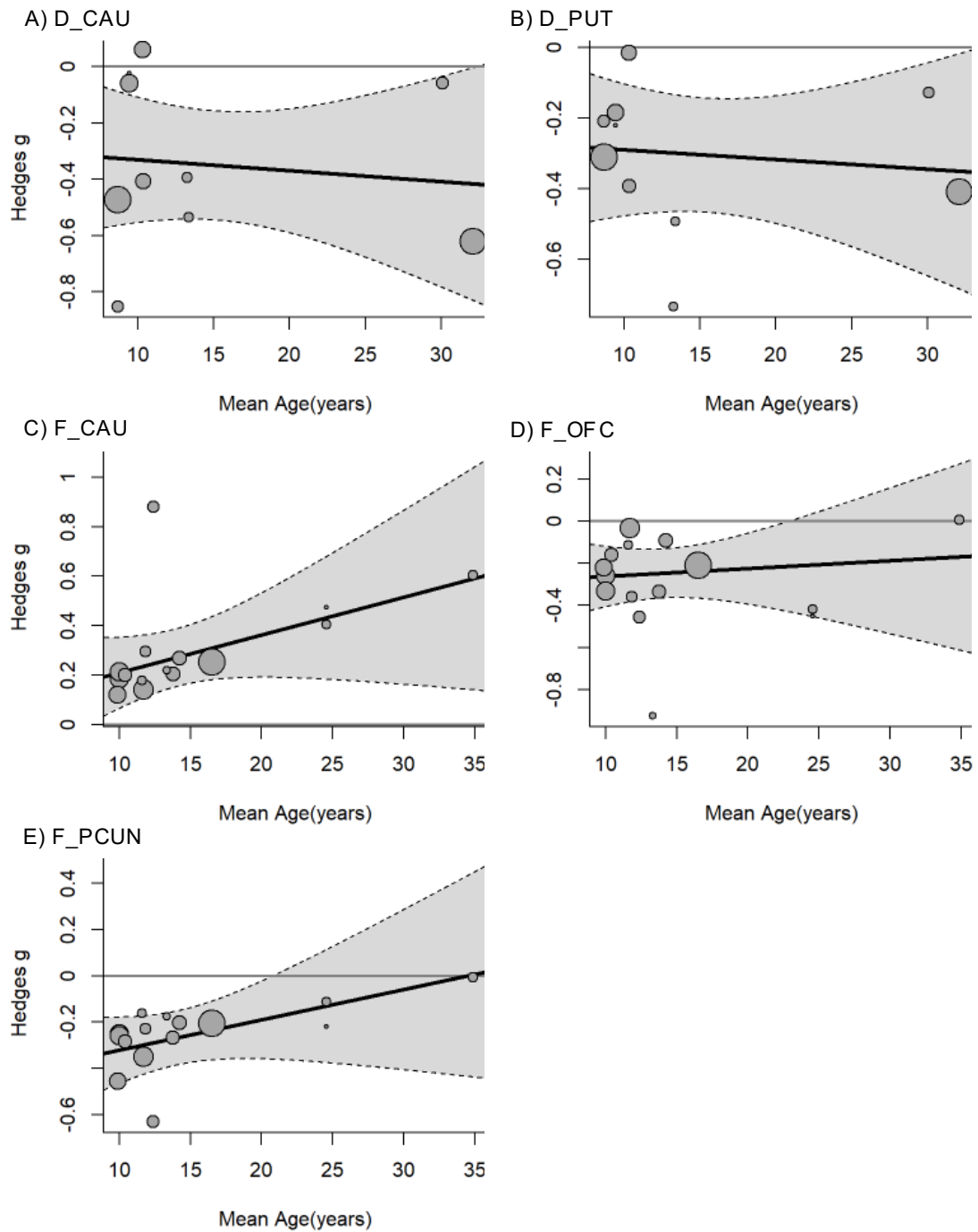
(A–E) Funnel plots of global efficiency, clustering coefficient, characteristic path length, modularity, and small worldness derived from dMRI. Visual inspection of the funnel plot suggested no evident asymmetry. (F–I) Funnel plots of global efficiency, clustering coefficient, characteristic path length, and modularity derived from fMRI. Visual inspection of the funnel plot suggested no evident asymmetry.

Figure S3. Leave-one-out Influence Analysis of Global Topological Metrics



(A–E) Leave-one-out analyses of global efficiency, clustering coefficient, characteristic path length, modularity, and small worldness derived from dMRI. The result of modularity reached statistical significance after the removal of one study. (F–I) Leave-one-out analyses of global efficiency, clustering coefficient, characteristic path length, and modularity derived from fMRI. The pooled effect sizes of characteristic path length and modularity become significant after the removal of one study in each case.

Figure S4. Meta-regression of local Metric Effect Sizes on Mean Age



(A–B) Bubble plots showing the meta-regression of effect sizes for dMRI hubness alterations against the mean age of study populations. The regions include (A) Caudate ($\beta = -0.004$, $p = .72$) and (B) Putamen ($\beta = -0.003$, $p = .76$). (C–E) Bubble plots showing the meta-regression of effect sizes for fMRI hubness alterations against the mean age of study populations. The regions include (C) Caudate ($\beta = 0.015$, $p = .15$), (D) Orbitofrontal Cortex ($\beta = 0.004$, $p = .72$), and (E) Precuneus ($\beta = 0.013$, $p = .21$). Note. The solid line represents

the fitted regression line, and the shaded area indicates the 95% confidence interval. Circle size reflects the weight of each study in the meta-analysis.

Table S1. Definition of Topological Metrics

Metric	Interpretation	Binary Definition	Weighted Definition
Nodal Metric			
k_i (Degree)	Nodal centrality based on the number (or total weight) of its connections. High values identify potential hubs (van den Heuvel & Sporns, 2013).	$k_i = \sum_{j \in N} a_{ij}$ a_{ij} is the connection status (1 or 0) between nodes i and j .	$k_i^w = \sum_{j \in N} w_{ij}$ w_{ij} is the connection weight between nodes i and j .
E_i (Nodal Efficiency)	Efficiency of information transfer from node i to all other nodes (Achard & Bullmore, 2007).	$E_i = \frac{1}{n-1} \sum_{j \in N, j \neq i} d_{ij}^{-1}$ Average inverse shortest path length specifically for node i .	$E_i^w = \frac{1}{n-1} \sum_{j \in N, j \neq i} (d_{ij}^w)^{-1}$ Average inverse weighted shortest path length specifically for node i .
Global Metric			
Lp (Characteristic Path Length)	The average minimum number (or weight) of steps required for information to flow between any two nodes. Indicates the network's capacity for global integration.	$Lp = \frac{1}{n} \sum_{i \in N} \frac{\sum_{j \in N, j \neq i} d_{ij}}{n-1}$ n is the number of nodes; d_{ij} is the shortest path length between nodes i and j .	$Lp^w = \frac{1}{n} \sum_{i \in N} \frac{\sum_{j \in N, j \neq i} d_{ij}^w}{n-1}$ d_{ij}^w is the shortest weighted path length.
E_{glob} (Global Efficiency)	The average efficiency of parallel information transfer between all pairs of nodes. Robust to disconnected networks; higher values indicate greater integration (Achard & Bullmore, 2007).	$E_{glob} = \frac{1}{n} \sum_{i \in N} \frac{\sum_{j \in N, j \neq i} d_{ij}^{-1}}{n-1}$ d_{ij}^{-1} is the inverse of the shortest path; handles disconnected nodes ($1/\infty = 0$).	$E_{glob}^w = \frac{1}{n} \sum_{i \in N} \frac{\sum_{j \in N, j \neq i} (d_{ij}^w)^{-1}}{n-1}$ Uses inverse weighted shortest paths to represent communication efficiency.

C_p (Clustering Coefficient)	<p>The probability that the neighbors of a node are also connected to each other. Quantifies the prevalence of local cliques or functional segregation.</p>	$C_p = \frac{1}{n} \sum_{i \in N} \frac{2t_i}{k_i(k_i - 1)}$ <p>t_i is the number of triangles around node i.</p>	$C_p^w = \frac{1}{n} \sum_{i \in N} \frac{2t_i^w}{k_i(k_i - 1)}$ <p>t_i^w is the weighted geometric mean of triangles around node i.</p>
Q (Modularity)	<p>The degree to which the network is organized into distinct, non-overlapping communities. Positive values indicate that within-module connections are denser than expected in a random network.</p>	$Q = \frac{1}{l} \sum_{i,j \in N} \left[a_{ij} - \frac{k_i k_j}{l} \right] \delta(m_i, m_j)$ <p>l is the total number of edges; $\delta(m_i, m_j) = 1$ if nodes belong to the same module, 0 otherwise.</p>	$Q^w = \frac{1}{l^w} \sum_{i,j \in N} \left[w_{ij} - \frac{k_i^w k_j^w}{l^w} \right] \delta(m_i, m_j)$ <p>l^w is the sum of all weights in the network.</p>
σ (Small-worldness)	<p>A summary statistic indicating whether a network combines high local clustering (segregation) with short path lengths (integration). $\sigma > 1$ suggest a small-world organization (Humphries & Gurney, 2008).</p>	$\sigma = \frac{C_p / C_{p_{rand}}}{L_p / L_{p_{rand}}}$ <p>$C_{p_{rand}}$ and $L_{p_{rand}}$ are mean metrics from a population of randomized null-model networks.</p>	$\sigma^w = \frac{C_p^w / C_{p_{rand}}^w}{L_p^w / L_{p_{rand}}^w}$ <p>Normalized against weighted null-model networks.</p>

Note: Unless otherwise specified, definition of metrics follow Rubinov & Sporns (2010) and Latora & Marchiori (2001). The formulas above are for undirected networks in both binary and weighted cases; further details regarding calculations for directed networks can be found in Rubinov & Sporns (2010).

Table S2. Quality Assessment of Included Studies

Study	Metric Level	Subjects				Image acquisition and analysis					Results and conclusions			Total score
		# 1	# 2	# 3	# 4	# 1	# 2	# 3	# 4	# 5	# 1	# 2	# 3	
dMRI														
Cao (2013)	both	1	1	1	1	1	1	1	0.5	1	1	1	1	11.5
Çelik (2020)	both	1	1	0.5	1	1	1	1	1	1	1	1	1	11.5
Griffiths (2021)	both	1	1	1	1	1	1	1	0.5	1	1	1	1	11.5
Sidlauskaite (2015)	both	1	1	1	1	1	1	1	1	1	1	1	1	8.5
Tolonen (2023)	both	1	1	1	1	1	1	1	0	1	1	1	1	11
Wang (2021)	both	1	1	0.5	1	1	1	1	0.5	1	1	1	1	11
Wu (2024)	both	1	1	1	1	1	1	1	0.5	1	1	1	1	11.5
Beare (2017)	nodal	1	1	0.5	1	1	1	1	0	0.5	1	1	1	10
Qian (2021)	nodal	1	1	0.5	0.5	1	1	1	0.5	0.5	1	1	1	10
Saad (2021)	nodal	1	1	1	1	1	1	1	1	0.5	1	1	1	11.5
Schulze (2023)	nodal	1	1	0.5	1	1	1	1	0.5	0.5	1	1	1	10.5
Soman (2023)	nodal	0.5	0.5	1	0.5	1	0.5	0.5	0	0.5	1	1	1	8
He (2022)	global	0.5	0.5	0.5	1	1	0.5	0.5	0.5	0.5	1	1	1	8.5
Ohnishi (2023)	global	1	1	1	1	1	1	1	0.5	0.5	1	1	1	11.5
fMRI														
Chen (2019)	both	1	1	1	1	1	1	1	0.5	1	1	1	1	11.5
Lin (2013)	both	1	1	0	1	1	1	1	1	1	0	1	1	10
Qin (2024)	both	1	1	1	1	1	1	1	0.5	1	1	1	1	11.5
Hong (2017)	nodal	1	1	1	1	1	1	1	1	0.5	0	1	1	10.5
Kyeong (2017)	nodal	1	1	0.5	1	1	1	1	1	0.5	1	1	1	11
Luo (2018)	nodal	1	1	1	1	1	1	1	0	0.5	1	1	1	10.5

Martino (2013)	nodal	1	1	1	1	1	1	1	1	0.5	1	1	1	11.5
Rezaei (2022)	nodal	1	1	0	1	1	1	1	1	0.5	1	1	1	10.5
Saad (2022)	nodal	1	1	1	1	1	1	1	1	0.5	1	1	1	11.5
Soman (2023)	nodal	0.5	0.5	1	0.5	1	1	1	0	0.5	1	1	1	9
Wang (2009)	nodal	1	1	0	1	1	1	1	0.5	0.5	0	1	1	9
Xia (2014)	nodal	1	1	1	1	1	1	1	1	0.5	1	1	1	11.5
Yao (2014)	nodal	1	1	0.5	1	1	1	1	0.5	0.5	0	1	1	9.5
Qian (2019)	global	1	1	1	1	1	1	1	1	0.5	1	1	1	11.5
Sato (2013)	global	1	1	0	1	1	1	1	0.5	0.5	1	1	1	10
Tao (2017)	global	1	1	1	1	1	1	1	0	0.5	1	1	1	10.5
Wang (2020)	global	1	1	0.5	1	1	1	1	1	0.5	1	1	1	11

Table S3. Sensitivity Analysis of Variance Estimators for Global Metric Pooling

Metric	Model	ES	LC	UC	τ^2	ρ^2	Q	<i>p</i>
dMRI								
Eg	PM	-0.30	-0.54	-0.07	0.04	40.02%	11.60	.114
	REML	-0.31	-0.54	-0.07	0.04	39.07%	11.60	.114
Cp	PM	0.05	-0.24	0.34	0.08	51.61%	9.55	.145
	REML	0.10	-0.10	0.29	0.00	0.00%	9.55	.145
Lp	PM	0.15	-0.11	0.41	0.07	53.53%	15.95	.026
	REML	0.15	-0.12	0.42	0.08	56.16%	15.95	.026
Q	PM	-0.25	-0.77	0.28	0.22	78.46%	14.76	.002
	REML	-0.25	-0.78	0.28	0.22	78.75%	14.76	.002
σ	PM	0.03	-0.24	0.30	0.02	23.18%	5.44	.246
	REML	0.02	-0.27	0.31	0.03	31.52%	5.44	.246
fMRI								
Eg	PM	-0.09	-0.40	0.22	0.08	66.79%	8.72	.069
	REML	-0.09	-0.35	0.17	0.05	53.99%	8.72	.069
Cp	PM	0.13	-0.47	0.73	0.25	92.17%	9.83	.007
	REML	0.13	-0.44	0.69	0.21	91.15%	9.83	.007
Lp	PM	0.12	-0.15	0.39	0.06	71.88%	11.89	.018
	REML	0.12	-0.13	0.37	0.05	66.75%	11.89	.018
Q	PM	-0.07	-0.98	0.83	0.56	88.07%	15.32	.001
	REML	-0.07	-0.97	0.82	0.55	87.92%	15.32	.001

Abbreviation: dMRI, diffusion magnetic resonance imaging; fMRI, functional magnetic resonance imaging, PM, Paule-Mandel method; REML, restricted maximum likelihood; ES, pooled effect size; LC, lower confidence limit; UC, upper confidence limit. Note: Aside from global efficiency, no other metrics yielded a significant pooled effect size across both variance estimator models. τ^2 and ρ^2 varied across models, but Q and corresponding *p*-value remain consistent.

Table S4. Funnel Plots and Bias Analyses in Regions with Hubness Alteration

Regions	Peak coordinates (x, y, z)	Symmetry of Funnel plot	Egger's test		Excess significance test
			<i>Bias</i>	<i>p</i>	<i>p</i>
Functional Connectome					
L Caudate	-10, 8, 14	Yes	0.01	.992	.897
R Orbitofrontal Cortex	6, 50, -4	No	0.01	.995	.999
L Precuneus	-8, -58, 48	Yes	0.01	.991	.831
Structural Connectome					
L Caudate	-12,12,10	No	0.03	.988	.262
R Putamen	28, 2, 2	No	0.02	.992	.485

Note. A p-value < .10 in the Egger's test is considered indicative of potential asymmetry in the funnel plot, suggesting possible small-study effects or publication bias. A p-value < .05 in the excess significance test indicates that the number of statistically significant findings may be greater than expected, suggesting potential selective reporting or publication bias. Abbreviations: L, left; R, right.